# Supporting Information

## Mitrea et al. 10.1073/pnas.0907668107

### SI Text

**Characterization of Bn-AFF-67.** We also created the AFF construct in which amino acids 67–110 of Bn were duplicated and appended to the N-terminus with an 18-residue linker ($(GGS)_5GTM$). The IFLETS sequence (plus flanking residues as described in the text) was inserted between Lys66-Ser67 of F1 and the H102A mutation was introduced into F1. This construct is designated Bn-AFF-67. We additionally made F1 and F2 analogs. Bn-F1-67 consists of WT Bn with the IFLETS insertion and the H102A mutation. Bn-F2-67 is WT Bn circularly permuted at position 67 with the aforementioned peptide linking the original N- and C-termini.

CD spectra of Bn-F1-67 and Bn-F2-67 are similar to each other and to the CD spectra of Bn-F1 and Bn-F2 (Fig. S3). All species exhibit the 231 nm minimum which is characteristic of WT Bn. The stabilities of Bn-F1-67 ($\Delta G^{H2O} = 6.4 \pm 0.4$) and Bn-F2-67 ($\Delta G^{H2O} = 5.3 \pm 0.4$), as determined by equilibrium urea denaturation experiments, are very similar to those of Bn-F1 and Bn-F2, respectively (Table S1). Consequently, Bn-AFF-67 is expected to primarily adopt the F1 conformation. In support of that conclusion, the urea denaturation curve of Bn-AFF-67 is similar to that of Bn-F1-67 but not to that of Bn-F2-67 (Fig. S4). We further tested that hypothesis by introducing the W94K mutation into F1 of Bn-AFF-67. The W94K mutation destabilizes Bn-F1-67 by 1.6 kcal/mol (Table S1) and is therefore predicted to reverse the F2 $\leftrightarrows$ F1 equilibrium to favor F2. Bn-AFF-67(K94) displays the 231 nm CD minimum (Fig. S3) and its urea denaturation curve matches that of Bn-F2-67 (Fig. S4). These data indicate that the W94K mutation induces the fold shift from F1 to F2.

The difference in stability between Bn-F1-67 and Bn-F2-67 ($\Delta\Delta G^{H2O} = 1.1$ kcal/mol) implies that a substantial percentage of Bn-AFF-67 molecules will adopt the catalytically active F2 conformation. To minimize RNase activity of full-length Bn-AFF-67, we introduced the W94′K mutation into F2. This mutation is calculated to reduce the F2 population to $<10\%$ (Table 1). Thus, Bn-AFF-67(K94′) is the stability-optimized form of the position 67 AFF construct, in the same way that Bn-AFF(P94′) is the stability-optimized form of the position 93 construct.

An unexpected band (approximately 11 kDa) on SDS-PAGE was observed after cleaving Bn-AFF-67 with PR (Fig. S1). Subsequent mass spectral analysis identified this species to be the product of a second PR cleavage event at Trp94′. The sequence surrounding positions 94′ and 94 shares homology with known PR substrates (1) and both Bn-AFF-67 and Bn-AFF-67(K94′) undergo miscleavage. The secondary site appears to be exposed in F2 of Bn-AFF-67 but is protected from proteolysis when Bn is folded: PR does not cleave at Trp94 in WT Bn or any isolated F1 or F2 analog. This result is consistent with mass spectrometry data (Fig. 5 of accompanying paper) that suggest that the duplicated tails are unstructured. PR does not miscleave Bn-AFF(P94′) because Bn-AFF(P94′) lacks the P4 substrate binding site and Pro does not appear to be a preferred amino acid at the P1 position (1). Fig. S1 shows that approximately half of Bn-AFF-67 molecules become miscleaved. Because these molecules will be locked into F1 and unable to fold shift, we excluded PR-cleaved Bn-AFF-67 variants from further study.

**Materials and Methods.** ***Protein expression and purification.*** WT Bn, F1 and F2 analogs, and Bn-AFF variants were coexpressed with barstar in *E. coli* BL21(DE3) at 20 °C. These proteins were soluble and were purified as described (2). Bn-AFF-67 variants were expressed in inclusion bodies (37 °C) and were purified as follows. Cells were lysed and centrifuged, and the supernatant discarded. Pellets were washed repeatedly with 20 mM Tris (pH 7.5), 1 mM EDTA and the same buffer containing 0.5 M NaCl. Pellets were then dissolved in 9 M urea, 20 mM Tris (pH 7.5) to dissociate the Bn-AFF-67/barstar complex. The solution was passed through a DE52 column (Whatman) to remove barstar. The flow through was then dialyzed against double-distilled water and lyophilized. Proteins were judged to be approximately 95% pure by SDS-PAGE.

***Thermal denaturation experiments.*** Protein samples were prepared as described in the text. Thermal denaturation curves for Bn-F1 (3.6 μM), Bn-F2(P94) (6.7 μM), and PR-cleaved Bn-F1 (10 μM) were monitored by CD signal at 230 nm. Thermal denaturation of PR-cleaved Bn-F1 (1 μM) was monitored by Trp fluorescence because CD signal is too weak at that protein concentration. Unfolding was tracked by the change in the wavelength of maximum emission ($F_{max}$). $F_{max}$ changes from 335 nm in native Bn to 355 nm in unfolded Bn (3). $F_{max}$ values were obtained by fitting emission spectra using the Datamax software package (Horiba/Jobin-Yvon). $T_m$ values were calculated by fitting the data to the two-state unfolding model.


1 . Kontijevskis A, Wikberg JE, & Komorowski J (2007) Computational proteomics analysis of HIV-1 protease interactome. *Proteins* 68(1):305–312.

2 . Cutler T, Mills BM, Lubin DJ, Chong LT, & Loh SN (2009) Effect of interdomain linker length on an antagonistic folding-unfolding equilibrium between two protein domains. *J Mol Biol* 386:854–868.

3 . Radley TL, Markowska AI, Bettinger BT, Ha J-H, & Loh SN (2003) Allosteric switching by mutually exclusive folding of protein domains. *J Mol Biol* 332:529–536.

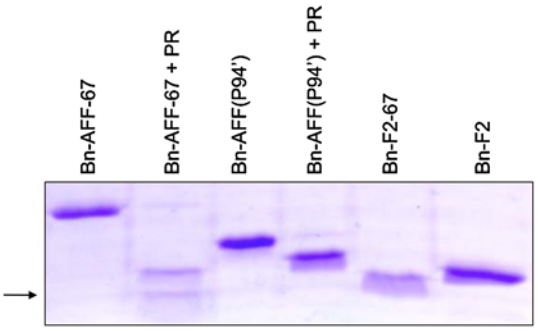


**Fig. S1.** PR cleavage of Bn-AFF variants assayed by 15% SDS-PAGE with staining by Coomassie Brilliant Blue. The arrow indicates the miscleaved product in the Bn-AFF-67 + PR lane.

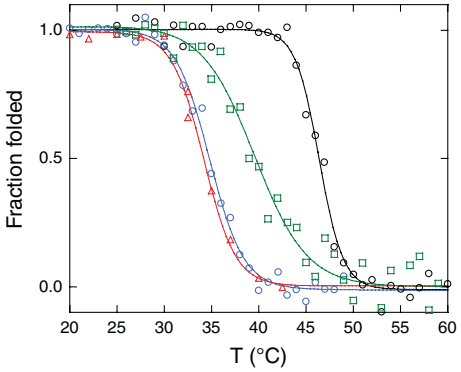


**Fig. S2.** Thermal denaturation curves of Bn-F1 (*Black Circles*), Bn-F2(P94) (*Green Squares*), PR-cleaved Bn-F1 at 10 μM concentration (*Blue Circles*), and PR-cleaved Bn-F1 at 1 μM concentration (*Red Triangles*). Lines are best fits of the data to the two-state unfolding model.

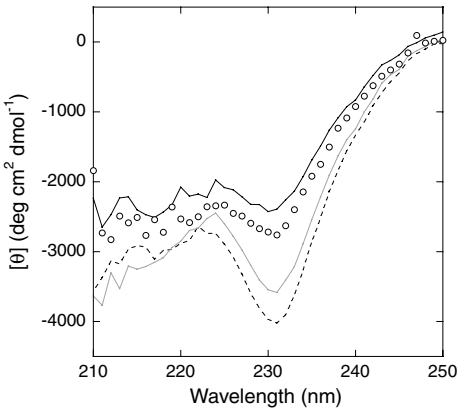


**Fig. S3.** CD spectra of Bn-AFF-67 and its F1 and F2 analogs. Lines are as follows: Bn-F1-67 (*Dashed*), Bn-F2-67 (*Gray*), Bn-AFF-67(K94′) (*Solid Black*), Bn-AFF-67 (K94) (*Circles*).

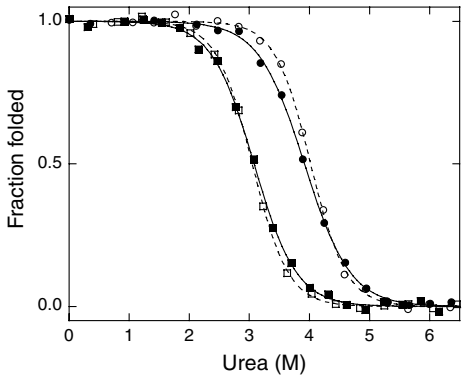


**Fig. S4.** Urea-induced denaturation of Bn-AFF-67 and associated variants, monitored by Trp fluorescence and normalized to fraction folded. Symbols are as follows: Bn-F1-67 (*Open Circles*), Bn-AFF-67 (*Closed Circles*), Bn-F2-67 (*Open Squares*), Bn-AFF-67(K94) (*Closed Squares*).

**Table S1. Thermodynamic parameters of Bn-AFF-67 and associated variants. Errors are standard deviations of at least three measurements.**

| F1 or F2 analog | $\Delta G^{H2O}$ (kcal/mol) | $m$ (kcal/mol/M) | $C_m$ (M) |
|---|---|---|---|
| WT Bn | $8.4 \pm 0.8$ | $1.8 \pm 0.2$ | $4.8 \pm 0.02$ |
| Bn-F1-67 | $6.4 \pm 0.4$ | $1.6 \pm 0.1$ | $3.9 \pm 0.03$ |
| Bn-F2-67 | $5.3 \pm 0.4$ | $1.8 \pm 0.1$ | $3.0 \pm 0.03$ |
| Bn-F1-67(K94) | $4.8 \pm 0.08$ | $2.1 \pm 0.03$ | $2.3 \pm 0.01$ |
| Bn-F2-67(K94) | $3.2 \pm 0.1$ | $2.2 \pm 0.04$ | $1.5 \pm 0.03$ |
| AFF variant | $\Delta G^{H2O}$ (kcal/mol) | $m$ (kcal/mol/M) | $C_m$ (M) |
| Bn-AFF-67 | $6.2 \pm 0.7$ | $1.6 \pm 0.1$ | $3.9 \pm 0.14$ |
| Bn-AFF-67(K94) | $4.9 \pm 0.07$ | $1.6 \pm 0.03$ | $3.1 \pm 0.02$ |
| Bn-AFF-67(K94′) | $9.1 \pm 1.2$ | $2.3 \pm 0.3$ | $4.0 \pm 0.04$ |